Development of ITER 15 MA ELMy H-mode Inductive Scenario

C. E. Kessel[1], D. Campbell[2], Y. Gribov[2], G. Saibene[3], G. Ambrosino[4], T. Casper[5], M. Cavinato[3], H. Fujieda[6], R. Hawryluk[1], L. D. Horton[7], A. Kavin[8], R. Kharyrutdinov[9], F. Koechl[10], J. Leuer[11], A. Loarte[2], P. J. Lomas[12], T. Luce[11], V. Lukash[13], M. Mattei[14], I. Nunes[15], V. Parail[12], A. Polevoi[2], A. Portone[3], R. Sartori[3], A.C.C. Sips[7], P. R. Thomas[3], A. Welander[11], J. Wesley[11]

[1] Princeton Plasma Physics Laboratory, P.O. Box 451, Princeton University, Princeton, USA.
[2] ITER Organization, Cadarache 13108 Saint Paul Lez Durance, France.
[3] FUSION FOR ENERGY, Joint Undertaking, 08019 Barcelona, Spain.
[4] Associazione Euratom-ENEA-CREATE, DIMET, Università degli Studi di Napoli, Italy.
[5] Lawrence Livermore National Laboratory, P.O. Box 808, Livermore, USA.
[6] Naka Fusion Institute, Japan Atomic Energy Agency, Japan.
[7] Max-Planck-Institut für Plasmaphysik, EURATOM-Association, D-85748, Garching, Germany.
[8] D. V. Efremov Research and Scientific Institute of Electrophysical Apparatus, St. Petersburg, Russia.
[9] TRINITI, Troitsk, M.reg., Russia.
[10] Association EURATOM-ÖAW/ATI, Vienna, Austria.
[11] General Atomics, P.O. Box 85608, San Diego, USA.
[12] EURATOM/UKAEA Fusion Association, Culham Science Centre, Abingdon OX14 3DB, UK.
[13] Nuclear Fusion Institute Russian Research Center, Kurchatov Institute, Moscow, Russia.
[14] Associazione Euratom-ENEA-CREATE, DIMET, Università degli Studi di Reggio Calabria, Italy.
[15] Euratom/IST Fusion Association, Centro de Fusao Nuclear, Lisboa, Portugal.
email: ckessel@pppl.gov

Abstract. The poloidal field (PF) coil system on ITER, which provides both feedforward and feedback control of plasma position, shape, and current, is a critical element for achieving mission performance. Analysis of PF capabilities has focused on the 15 MA Q = 10 scenario with a 300-500 s flattop burn phase. The operating space available for the 15 MA ELMy H-mode plasma discharges in ITER and upgrades to the PF coils or associated systems to establish confidence that ITER mission objectives can be reached have been identified. Time dependent self-consistent free-boundary calculations were performed to examine the impact of plasma variability, discharge programming, and plasma disturbances. Based on these calculations a new reference scenario was developed based upon a large bore initial plasma, early divertor transition, low level heating in L-mode, and a late H-mode onset. Equilibrium analyses for this scenario indicate that the original PF coil limitations do not allow low l_i (<0.8) operation or lower flux states, and the flattop burn durations were predicted to be less than the desired 400 s. This finding motivates the expansion of the operating space, considering several upgrade options to the PF coils. Analysis was also carried out to examine the feedback current reserve required in the CS and PF coils during a series of disturbances and a feasibility assessment of the 17 MA scenario was undertaken. Results of the studies show that the new scenario and modified PF system will allow a wide range of 15 MA 300-500 s operation and more limited but finite 17 MA operation.

1. Introduction

The poloidal field (PF) coil system on ITER[1] provides both feedforward and feedback control of the plasma position, shape, and current. These coils must provide a range of baseline plasma configurations that include the 15 MA Q=10 Inductive, 13.5 MA Hybrid, and 8-9 MA Steady State scenarios. Analysis to date has focused on the 15 MA scenario with a 300-500 s flattop burn phase, which is the ITER design basis and is the most challenging for the PF coils. In the course of producing a large range of plasmas, the PF coils must remain within all limits, which includes coil current limits, coil field limits, central solenoid force limits, an imbalance current on the outermost coils in the vertical position control loop, voltage and power limits, and allowances on the plasma to first wall

(FW) clearance and divertor strike point locations. Due to the high plasma current these constraints are challenging, yet at the same time ITER must be sufficiently flexible to allow for plasma parameter uncertainties, operator control requests, and a wide range of disturbances. Work reported here focused on identifying the operating space available for the 15 MA ELMy H-mode plasma discharges in ITER and upgrades to the PF coils or associated systems to improve confidence that the ITER mission can be reached.

The ITER PF coil system is shown in Fig. 1a, and consists of six central solenoid (CS) coils, and 6 outer coils. All coils are superconducting with independent 4 quadrant power supplies. The exceptions are the 2 centermost CS coils which are connected in series. All the coils participate in the feedback control of plasma position, shape, and current. In addition, the outer coils PF2, PF3, PF4 and PF5 are connected to a high voltage converter for the vertical position control.

The "nominal" 15 MA ELMy H-mode plasma is characterized by $I_P = 15$ MA, $B_T = 5.3$ T, $R = 6.2$ m, $a = 2.0$ m, $\kappa = 1.85$, $T_{e,i}(0) \approx 22$ keV, $T_{ped} \approx 5$ keV, $T(0)/<T>_v \approx 2.5$, $n_{20}(0) = 1.05$, $n(0)/<n>_v = 1.05$, $l_i(3) = 0.8$, $\beta_N = 1.8$, $P_\alpha = 80$ MW, $P_{aux} = 40$ MW. These are burn phase design parameters, the simultaneous achievement of which is uncertain. The plasmas produced in the rampup and rampdown of a discharge can be quite different from the flattop configuration.

Calculations of the plasma equilibrium were done to solve for PF coil currents given a range of plasma current profiles and flux states, using four independent codes [2(EQ1), 3(EQ2), 4(EQ3), 5(EQ4)]. The pressure of the 15 MA reference discharge is fixed at a $\beta_N \approx 1.8$, and has a weak influence on coil currents. The pressure and current profiles, however, must have the consistent shape associated with the H-mode pedestal. Time-dependent calculations with energy transport and bootstrap current were used to provide self-consistent profile combinations for $p(\psi)$ and $j_{\parallel}(\psi)$ for equilibrium analysis. It is found that the coil current solutions can be affected by the pedestal features, so a range of models is examined to account for the uncertainty in predicting the pedestal in ITER. The flux state is defined as the poloidal magnetic flux from all coils linked through a specified (R,Z) location (generally the major radius or magnetic axis) or linked over the entire plasma, the difference of which was found to be quite small. All of the codes constrain the locations of plasma boundary points, X-points, and strike points, and may also constrain poloidal flux differences, inactive X-points, and vertical plasma position.

Free-boundary transport evolution codes TSC, DINA, and Corsica [6,7,3] were used to examine the complete discharge evolution following breakdown and early startup. In these simulations feedback systems are used for plasma position, shape and current control, the plasma is grown from a limited plasma to a full size diverted plasma, the primary conducting structures are included, and the plasma equilibria are self-consistent with the plasma energy, particle and current transport. The primary use of these simulations is to examine actual discharge features, which are absent from equilibrium analysis, and investigate how they affect the PF coil currents and plasma evolution. Several variations have been examined including energy confinement assumption, Z_{eff}, plasma density, H-mode transition time, heating and divertor transition times, temperature pedestal height, and plasma current ramp rate.

2. 15 MA Scenario Analysis

Early simulations found that a superior rampup strategy could be used to avoid very peaked current profiles (high l_i) and strong vertical instability, while also allowing l_i to remain sufficiently high to avoid large PF coil currents, particularly in PF6. The plasma is initiated to have a large bore (minor radius between 1.7 and 2.0 m) at very early time, the plasma is grown and diverted early (approximately 10-15 s out of an 80-100 s I_P ramp), low level heating is initiated at the divertor transition time while keeping the plasma in L-mode, initiating the H-mode late in the I_P ramp (approximately 60-75 s in an 80-100 s I_P ramp). This approximate rampup procedure also avoids excessive volt-second consumption that occurs with strictly ohmic rampup, requiring from pre-magnetization about 202-225 V-s, depending on several variables, versus 250 V-s for ohmic rampup. This indicated that lower flux states were required at the start of burn to avoid saturation of the CS1 coil current, thereby saving enough volt-seconds for the long flattops required in ITER.
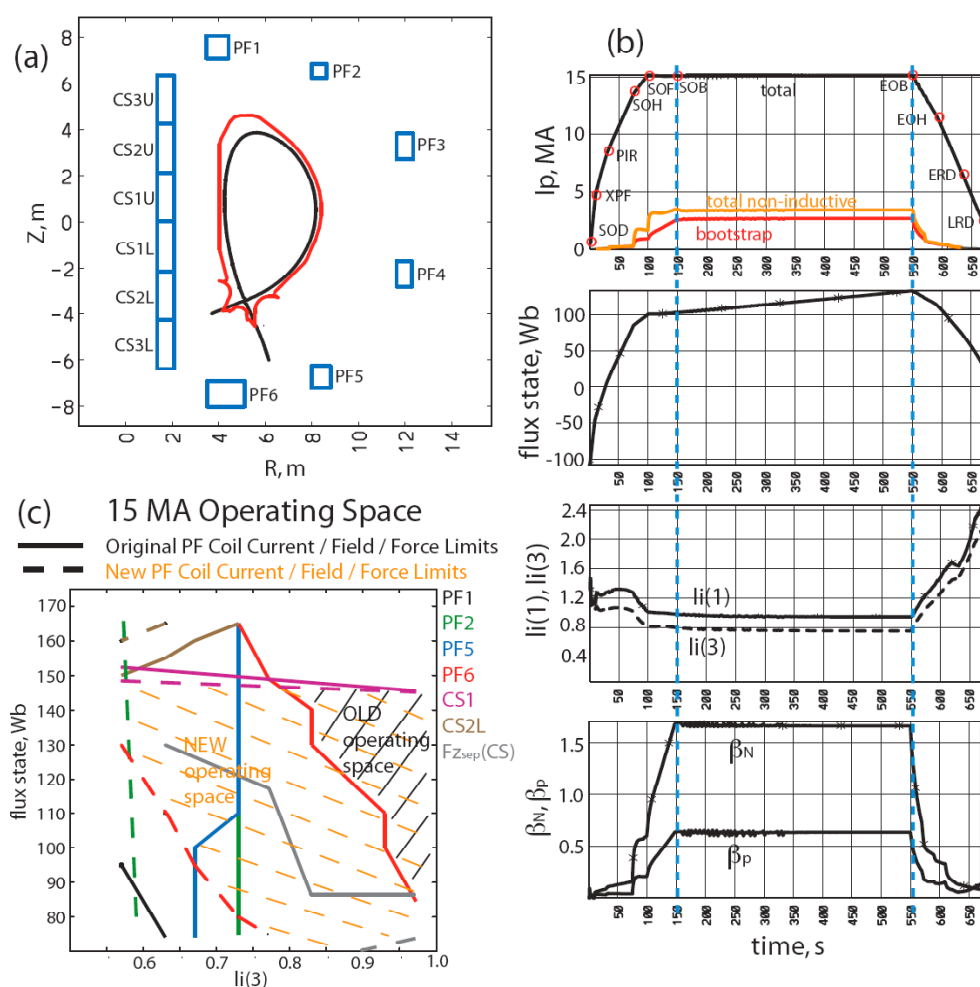

Figure 1. PF coil layout (a), Ip/flux state/li/β_N versus time for 15 MA discharge (b), flux state versus li operating space diagram showing OLD and NEW spaces with individual PF coil limits (c).

The discharge is broken into a series of phases and several fiducial points in the discharge are defined, such as X-point Formation (XPF), Start of Heating (SOH), Start of Flattop (SOF), Start of Burn (SOB), End of Burn (EOB), and End of Heating (EOH). Shown in Fig. 1b are the plasma current, plasma internal self-inductance (l_i), flux state, and β_N from a time-dependent simulation, denoting these points in the discharge. The primary focus has

been on the flattop burn phase bracketed by SOB to EOB, since it was found to be the most restrictive, while the current rampup and rampdown phases can take advantage of various techniques to control the l_i and flux state. Shown in Fig. 1c is a flux state vs $l_i(3)$ operating space diagram showing the region where various PF coils were within their limits. The available operating space is given by the hatched region, noted by "OLD operating space". It can be seen that the PF6 coil (current/field limit) is severely limiting access to the lower l_i and lower flux state region of the diagram, and that the CS1 (field limit) coil is limiting access to higher flux states at any l_i value. Examination of experimental discharges setup to imitate ITER discharges [8] showed that the $l_i(3)$ could reach values as low as 0.6-0.7 during the flattop, while code simulations of ITER discharges with pedestal temperatures ranging from 2.5-7.0 keV showed $l_i(3)$ values in the range of 0.88-0.62. This indicated that lower li plasmas were likely in ITER, and the PF coils must be able to produce and sustain them.

TABLE I. POLOIDAL FIELD COIL PARAMETERS

	Old Limits			New Limits		
	turns	I_{max}, MA	B_{max}, T	turns	I_{max}, MA	B_{max}, T
PF1	249	11.2	6.0	249	**12.0**	**6.4**
PF2	106	4.35	4.0	**116**	**6.38***	**4.8***
PF3	185	8.33	4.0	185	**10.2**	**4.8**
PF4	169	7.61	4.0	169	**9.30**	**4.8**
PF5	217	9.77	5.0	217	**11.3**	**5.7**
PF6	425	19.1	6.0	**460**	**23.9****	**6.8****
CS3L	548	24.7/21.9	12.6/13.0	548	24.7/21.9	12.6/13.0
CS2L	548	24.7/21.9	12.6/13.0	548	24.7/21.9	12.6/13.0
CS1L	548	24.7/21.9	12.6/13.0	548	24.7/21.9	12.6/13.0
CS1U	548	24.7/21.9	12.6/13.0	548	24.7/21.9	12.6/13.0
CS2U	548	24.7/21.9	12.6/13.0	548	24.7/21.9	12.6/13.0
CS3U	548	24.7/21.9	12.6/13.0	548	24.7/21.9	12.6/13.0

*includes resizing of PF2 from 106 to 116 turns
**includes relocation, resizing of PF6 from 425 to 460 turns, and also includes subcooling by 0.4 K (PF6 current limit without subcooling is 22.0 MA)
*** vertical forces on CS coils, F_Z^{sep}(old) < 75 MN, **F_Z^{sep}(new) < 120 MN**, F_Z^{net}(old=new) < 40 MN.

Based on these simulations and experimental results, upgrades were sought to expand the operating space to the lower l_i and lower flux state region. Expansion toward higher flux states was severely limited due to geometry constraints and force limits on the CS coils. Several upgrades were introduced to achieve this. Projection of improved superconductor performance, subsequently confirmed by R&D results [9], allowed proposals for upgrading of the current and field capacity of all the outer PF coils, while the CS coil current and field limits remained the same. In addition, the vertical separating force limit on the CS coils was increased from 75 to 120 MN after detailed analysis showed that the higher value could be tolerated before the separation distance between CS2L and CS3L was too high. The PF coil current and field maximum values before and after this update are given in Table I. In addition, the PF6 coil was expanded towards the plasma, which helped to reduce this coil's current with low l_i plasmas. It was found that modifying the inboard strike flux line could further reduce PF6 and other PF coil currents, so a re-designed divertor emerged [10], and allowed operation over a large operating space of l_i and flux state. The expansion of the operating space from the original PF coil configuration to the new one is shown in Fig. 1c, noted by "NEW operating space". The individual PF coils or CS force that limit the space are shown. The flattop operating space has been expanded significantly and can now accommodate a wide range of plasma configurations, with > 300 s flattop durations.

The equilibrium analysis has identified two possible ways of expanding the operating space further. The upper flux state limit can be increased by allowing the plasma boundary to deform on the inboard side toward the first wall. A maximum of 15-20 V-s can be gained by this technique. The primary concern with this is whether the proximity of the plasma to the first wall gives a higher probability of contact under certain disturbances. Therefore there may be an acceptable boundary deformation, but not as large as that identified.
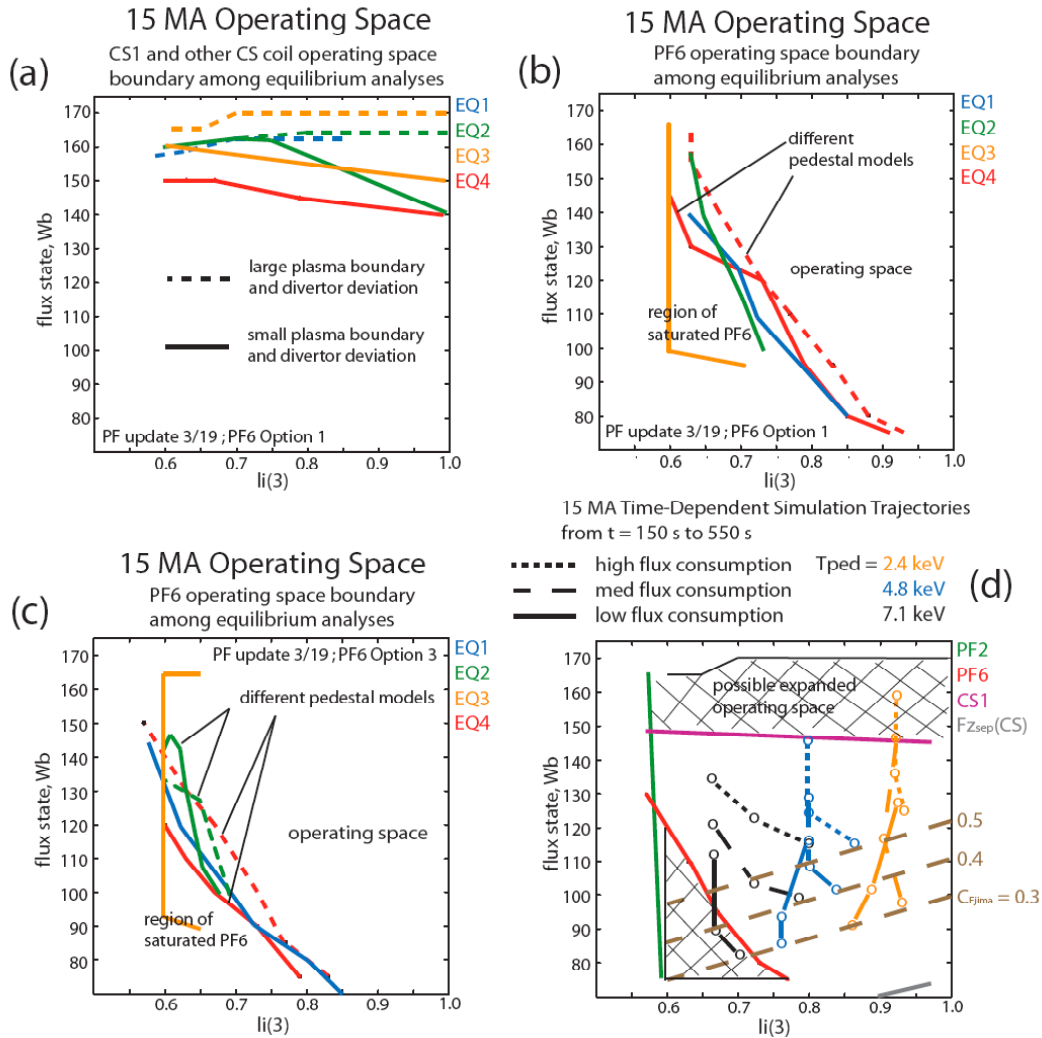
Figure 2. Flux state versus li operating space diagrams for CS1 upper flux state boundary (a), PF6 low flux state low li boundary for 2 different PF6 upgrades options (b) & (c), and including time-dependent simulation trajectories over a range of pedestal and flux consumption conditions (d).

Shown in Fig. 2a are the operating space boundaries associated with the high flux limit from the CS coils from the four equilibrium analyses. The additional flux swing from the plasma boundary deformation is significant, amounting to approximately 150 to 200 s of additional flattop time. The low l_i and low flux state corner of operating space can be expanded by allowing the PF6 coil to approach its limit and then clamping its current there, removing it from the algorithm solving for coil currents to produce the plasma shape in the equilibrium calculation. This forces all of the other PF coils to change their currents to compensate, and yields deviations of the plasma boundary, in some cases as high as 20 cm. In an actual discharge on ITER this would be done by removing PF6 from the feedback control, and proceeding with the discharge using only the other coils for feedback control. This is referred to as saturation control. It is not clear if the PF coil system has the capability

to operate under these conditions, in particular it may lead to a cascade of coils saturating one after the other if they are also near their limits. In addition, due to the resulting plasma boundary deformations, this approach may lead to a higher probability of FW contact during disturbances. Shown in Fig. 2b and c are the operating space boundaries for PF6 from the four equilibrium analyses for 2 different upgrade options to PF6. The agreement among the codes is relatively good, although the analysis with saturated PF6 can provide an enlargement to the operating space. Both of these methods will be studied in the future to identify their viability for expanding the operating space.

A systematic verification of the equilibrium operating space was done with time-dependent simulations by scanning the temperature pedestal height from 2.4 to 7.1 keV, which varies the l_i value, and scanning the energy confinement assumption, Z_{eff}, and applied power during the rampup, which varies the rampup flux consumption prior to SOB. An example of this is shown in Fig. 2d, where 9 separate cases are plotted from SOB to EOB on the NEW equilibrium operating space diagram from Fig. 1c. Also shown are the possible regions for expanded operation. These simulations have used pre-programmed CS3L current to avoid the CS separating force limit discussed below. All cases remain within the PF coil limits, except the lowest flux consumption and lowest l_i combination case, which can be seen to exceed the PF6 current/field limit. The cases show that the expansion of the operating space toward low l_i and low flux state allows most of the high and medium pedestal cases to remain within coil limits. At the high flux state region, the high l_i combined with high flux consumption exceeds the CS1 coil field limit, restricting the flattop burn to 150 s. By utilizing the plasma boundary expansion toward the inboard first wall, ≥ 300 s flattop times can be recovered. These time-dependent simulations with feedback control of the plasma and self-consistent equilibrium and transport evolution are confirming the operating space established with equilibrium analysis.

Several disturbances were identified as providing sufficiently large current requirements on the PF coils that they should be taken account in determining the operating space for the 15 MA reference scenario. The purpose of determining the current requirements for these disturbances is to subtract this transient current from the maximum PF coil current to establish an operating maximum current on each coil, guaranteeing that the disturbances can be rejected in any part of the discharge. This is referred to as feedback current reserve. The disturbances included and where they occur in the discharge are 1) H to L transition (SOB-EOB), 2) L to H transition (SOF-SOB), 3) vertical displacement event (VDE, XPF-EOH), 4) minor disruption (XPF-SOF,EOB-EOH), and 5) large ELM (SOF-SOB). Time dependent simulations were done using the prescribed changes in the current profile, stored energy, confinement regime, and density/temperature/pressure profiles based on experiments in JET, DIII-D, and ASDEX-U, and scaled to ITER parameters. A feedback controller typical of the modern optimal type (linear-quadratic-gaussian, LQG), designed for the ITER PF coils and conducting structures, was used for the control in the simulations.

The impact of the feedback current reserve on the operating space can be seen in Fig. 3a, where the diagram for the SOB to EOB phase of the discharge is given with the feedback reserve included. The solid lines correspond to using the flattop reserve with very small deviations from the nominal plasma boundary, while the dashed lines assume the maximum reserve and has allowed somewhat larger deviations (5 cm). Although the maximum reserve is not appropriate for the flattop phase of the discharge, it is still examined as a limiting case due to the uncertainty in the disturbance specifications. The time-dependent trajectories with different pedestals and flux consumption in the current rampup from Fig. 2d, show that

the primary impact for the flattop phase of the discharge is a lower maximum flux state boundary, which would reduce the available flattop time for some of the high and medium l_i plasmas. Allowing plasma boundary deviations of up to 5 cm on the inboard side of the
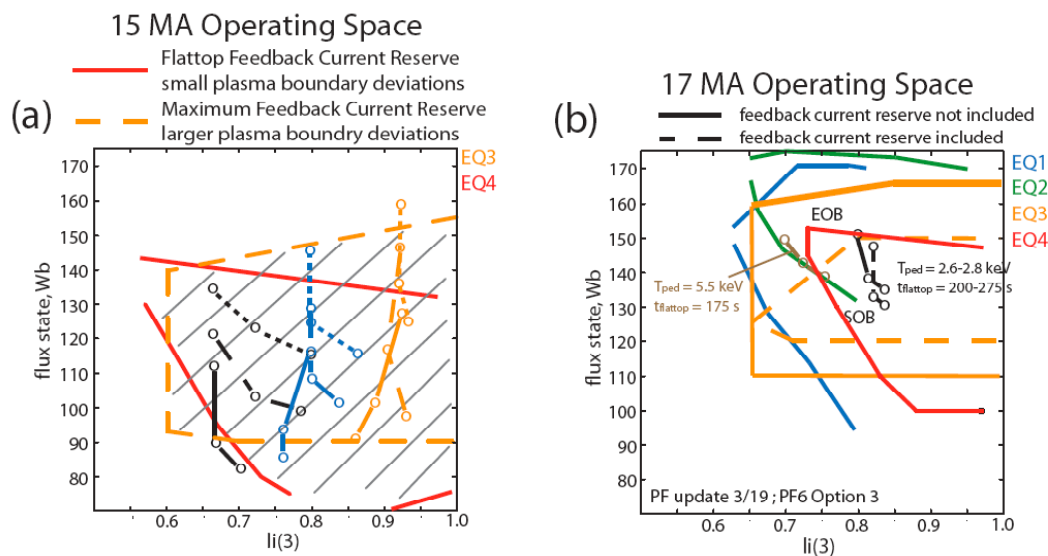

Figure 3. Flux state versus li operating space diagrams including flattop and maximum feedback current reserve (a), and 17 MA scenario (b).

plasma allows this boundary to be higher. The disturbance affecting the lower left boundary of the operating space, which is dominated by PF6, is the L to H transition, which is not considered a flattop disturbance. Although this is typically a part of the preprogrammed discharge evolution, and would not normally be considered a disturbance, unexpected drops out of the H-mode followed by re-entry to the H-mode may need to be treated in some form. Work is continuing to establish appropriate disturbances, their prescriptions for ITER, and the phases of the discharge where they may occur.

The time-dependent simulations have shown a much stronger sensitivity of the vertical separation force on the CS than appeared in the equilibrium calculations. In fact, multiple simulations have shown that this force criteria is exceeded over a wide range in the operating space, even though the equilibrium analysis showed that the limit could be avoided. The feedback systems for the plasma position, shape and current in the simulations are causing the CS3L coil current to remain high and positive during the discharge, which causes a higher separating force. The solution found has been to force the CS3L coil current along a pre-programmed trajectory, removing it from the feedback system. This allows a more precise control of this force on the CS, and in many ways is preferable to allowing the feedback system to determine this coil's current independent of the force constraints. The impact on the accuracy of the plasma shape and strike point control has been shown to be small. It is expected that an algorithm that monitors all the PF coil's parameters in real-time will be necessary during an ITER discharge, and integrating this with the plasma controller will be work for the future.

3. 17 MA Scenario

Shown in Fig. 3b is the flux state versus $l_i(3)$ operating space diagram for the possible extension to 17 MA, which is not part of the ITER baseline. As before with the 15 MA scenario, the four different equilibrium calculations used here result in some variation of the

operating space. Overall the space is smaller than the 15 MA case, accessing $l_i(3)$ values only as low as 0.65-0.75 and flux values from 110 to 175 Wb. The upper limit in flux state has taken advantage of an expansion of the plasma toward the inboard wall. In addition, the lowest l_i and lowest flux state corner (EQ3) has taken advantage of PF6 being held at its maximum current, while adjusting the other coils (saturation control). The dashed line shows the impact of control headroom, where the feedback current reserve has been scaled by 17/15, which severely shrinks the operating space. Time dependent analysis, using an 80 s I_P rampup, indicates that a flattop of approximately 200 s is achievable, although more analysis is required to map out the trajectories under varying plasma conditions.

4. Summary and Conclusions

Examination of the plasma operating space for the ITER 15 MA ELMy H-mode Inductive discharge indicated that the PF coils could not support a wide enough range of plasmas to give confidence that the mission goals could be met. Both equilibrium and time-dependent analysis, augmented by experimental information, was performed to identify how the operating space could be enlarged. Based on these, and with guidance from the IO Magnet and Physics divisions 1) the current/field capabilities for all PF coils were increased, 2) the CS separation force limit was increased, 3) PF6 was relocated and enlarged, and 4) the divertor inboard slot and dome have been redesigned. As a result of the analysis and accompanying redesign and R&D activities, the 15 MA operating space has been considerably expanded to reflect requirements established by the latest tokamak research. There is now confidence that the device has extensive capability for 15 MA long pulse operation in ELMy H-mode, with the potential for extension to 17 MA operation. Detailed analysis is continuing to examine a wide range of plasma scenarios, the prescription of disturbances for feedback current reserve, the rampdown phase, heating and current drive sources in the rampup, and to highlight operational questions which would benefit from experiments in present tokamaks.

References
[1] Progress in ITER Physics Basis Nuc. Fus. **47** (2007) S385; ITER Physics Basis Nuc. Fus. **39** (1999) 2137.
[2] H. Fujieda, et al, JAERI-M 08-256, 1996.; JA Team Physics Tasks for JAERI 2005, N19TD12FJ, March 2006.
[3] J. A. Crotinger, LL. Lodestro, L. D. Pearlstein, et al LLNL Report UCRL-ID-126284, 1997, NTIS #PB2005-102154; T. Casper, et al Fus. Engr. Des. **83** (2008) 552.
[4] R. Albanese, et al, Intl Symposium on Appl Electro. Mech. ISEM 2003, Versailles, France.; G. Ambrosino et al Fus. Engr. Des. **74** (2005) 521; M. Mattei, et al submitted to Fus. Engr. Des. (2008).
[5] C. E. Kessel, et al Fus. Engr. Des. **80** (2006) 63.
[6] S. C. Jardin, et al J.Comp Phys **66** (1986) 481; C. E. Kessel, et al Nuc. Fus **47** (2007) 1274.
[7] R.R. Khayrutdinov and V. E. Lukash, J. Comp. Phys. **109** (1993) 193.;V. E. Lukash et al, Plas. Dev. Op. **13** (2005) 143.
[8] A. C. C. Sips at this conference, IT/2-2
[9] D. Bessette, et al, Applied Superconductivity Conf., Chicago, Aug 2008, IEEE Trans. of Appl. Supercond.
[10] C. G. Lowry, this conference, IT/1-4; A. S. Kikushkin, this conference, IT/P6-15.